

## Dynamics of Coherent Anharmonic Phonons in Bismuth Using High Density Photoexcitation

Muneaki Hase,<sup>1\*</sup> Masahiro Kitajima,<sup>1</sup> Shin-ichi Nakashima,<sup>2</sup> and Kohji Mizoguchi<sup>3</sup>

<sup>1</sup>Materials Engineering Laboratory, National Institute for Materials Science, 1-2-1 Sengen, Tsukuba, Ibaraki 305-0047, Japan

<sup>2</sup>Power Electronic Research Center, National Institute of Advanced Industrial Science and Technology, 1-1-1 Higashi, Tsukuba, Ibaraki 305-8561, Japan

<sup>3</sup>Department of Applied Physics, Osaka City University, 3-3-138 Sugimoto, Sumiyoshi-ku, Osaka 558-8585, Japan

(Received 27 August 2001; published 24 January 2002)

We have investigated the dynamical properties of the coherent anharmonic phonons generated in Bi under high density excitation. The time-resolved reflectivity in the intensely photoexcited Bi film is modulated by the coherent  $A_{1g}$  phonon oscillation with a time-dependent oscillation period. As the pump power density is increased, the line shape of the  $A_{1g}$  mode in the Fourier transformed spectra becomes asymmetric, and the redshift of the phonon frequency is observed. Analysis of the transient redshift with a wavelet transform reveals that the frequency of the  $A_{1g}$  mode depends on the squared amplitude of the oscillation, which is attributed to an anharmonicity of the lattice potential.

DOI: 10.1103/PhysRevLett.88.067401

PACS numbers: 78.47.+p, 63.20.Ry, 78.66.Bz

High density excitation of materials with amplified femtosecond laser pulses has led to unique physical phenomena, such as femtosecond laser ablation and laser-induced phase transition [1–3]. These phenomena in narrow band-gap materials are considered to be induced by the photoexcitation of electrons from bonding into antibonding states (electronic softening), which will lead to a large lattice distortion along the lattice potential [3,4]. The photoexcitation of electrons changes the equilibrium positions of the atoms; the atoms then oscillate around their new equilibrium positions, a mechanism known as displacive excitation of coherent phonons [5]. In the past decade, coherent phonons have been actively studied in a variety of materials from various viewpoints [5–9]. However, only a few investigations of coherent phonons have been performed under high density excitation [10–14]. Under high density excitation with several  $\text{mJ}/\text{cm}^2$ , the amplitude of the coherent lattice displacement could increase up to several percent of the lattice constant. In this condition, large amplitude coherent phonons would play an important role in structural modification. The purpose of this paper is to study the characteristic properties of the large amplitude coherent phonons under the anharmonic lattice potential; this is based on the classical mechanics [15] which indicates that the frequency of the anharmonic oscillator depends on the amplitude of the oscillation.

The coherent lattice vibrations excited under high intensity conditions in  $\text{LiTaO}_3$ , a ferroelectric crystal that is transparent to the visible and near-infrared light, have been studied by Brennan and Nelson [12]. They have observed overtones of the coherent lattice vibrations up to ninth order. However, a frequency shift of the phonon modes due to anharmonicity has not been observed. Hunsche *et al.* [11] have reported that in photoexcited tellurium the frequency of the coherent  $A_{1g}$  mode decreases linearly with increasing the pump power density. They have suggested that the origin of the frequency shift is the electronic softening, whereas the asymmetric line shape results from in-

homogeneity of the carrier density due to carrier diffusion. However, there has been no report on the time-resolved study of the coherent phonons with a transient redshift of the phonon frequency induced by the anharmonicity of the lattice potential.

This Letter reports on the dynamical properties of coherent anharmonic optical phonons under high density excitation of more than several  $\text{mJ}/\text{cm}^2$ . The time-domain signals in the intensely photoexcited Bi film indicate the coherent  $A_{1g}$  phonon oscillation, exhibiting a frequency which depends on the time after the irradiation by the pump pulse. It is found that the frequency is proportional to the squared amplitude of the coherent oscillation, which is attributed to a contribution from the cubic term of the anharmonic potential.

The bismuth films used in this paper were prepared by vacuum deposition on polished silicon substrates at room temperature. Their thickness was about 100 nm, and x-ray diffraction measurements showed that they were polycrystalline. A reflection-type pump-probe measurement was carried out at room temperature. Femtosecond seed pulses from a Ti:sapphire laser oscillator, operating at a wavelength of 800 nm with a pulse duration of about 70 fs, were amplified to a pulse energy of 500  $\mu\text{J}$  in a 1 kHz regenerative-amplifier system. After compensation of the amplifier dispersion, 120 fs pulses in duration were obtained. The pump and probe beams were focused on samples to a diameter of about 100  $\mu\text{m}$ . The pump power density was reduced with a neutral density filter to below 7.6  $\text{mJ}/\text{cm}^2$  to prevent damaging the sample or causing laser ablation. The probe pulse energy was also reduced and fixed at 0.3  $\text{mJ}/\text{cm}^2$ . We estimated from the linear absorption coefficient of  $6 \times 10^5 \text{ cm}^{-1}$  at 800 nm [16] that the photoexcited carrier density at the maximum pump power fluence of 7.6  $\text{mJ}/\text{cm}^2$  is  $3.0 \times 10^{21} \text{ cm}^{-3}$  at the sample surface, which is  $\sim 2\%$  of all the valence electrons in Bi [17]. In order to obtain only oscillatory components in the signal, the pump beam was modulated at 250 Hz

using an optical shaker, and the signal was detected by a lock-in amplifier. The transient isotropic reflectivity change  $\Delta R/R$  was recorded by changing the optical path length of the probe beam.

Figure 1 shows the transient reflectivity change obtained for pump power densities from 0.9 to 7.6 mJ/cm<sup>2</sup>. Large amplitude coherent phonons are observed in the time domain. The coherent phonon observed using unamplified seed pulses with a pump power density of 3.0  $\mu$ J/cm<sup>2</sup> is also shown at the bottom of Fig. 1 for reference. The period of the coherent oscillation at the lowest pump power density of 0.9 mJ/cm<sup>2</sup> is about 346 fs, which is slightly longer than that of the  $A_{1g}$  mode observed with the seed pulses ( $\approx$ 340 fs) [5–7]. As the pump power density is increased, the amplitude of the coherent  $A_{1g}$  phonon gradually increases and its decay time decreases. The maximum amplitude of the coherent  $A_{1g}$  mode in the reflectivity  $\Delta R/R_0$  was  $\sim$ 0.012 at 7.6 mJ/cm<sup>2</sup>, which is 3 times larger than that obtained for a Bi single crystal in Ref. [14]. The amplitude of the coherent lattice displacement estimated from the maximum excited carrier density of  $3.0 \times 10^{21}$  cm<sup>-3</sup> is  $\sim$ 1.3  $\times 10^{-2}$  nm [5]. This large displacement corresponds to 4.2% of the interatomic distance of the nearest neighbors at room temperature. According to the Lindeman melting criterion [18], melting of solids would occur when the displacement of each atom exceeds  $\sim$ 10% of the mean atomic radius, e.g., 9.2% for Bi [19]. The 4.2% displacement obtained in this paper is below the critical displacement.

Figure 2 shows the Fourier transformed (FT) spectra obtained from the time-domain data for different pump power

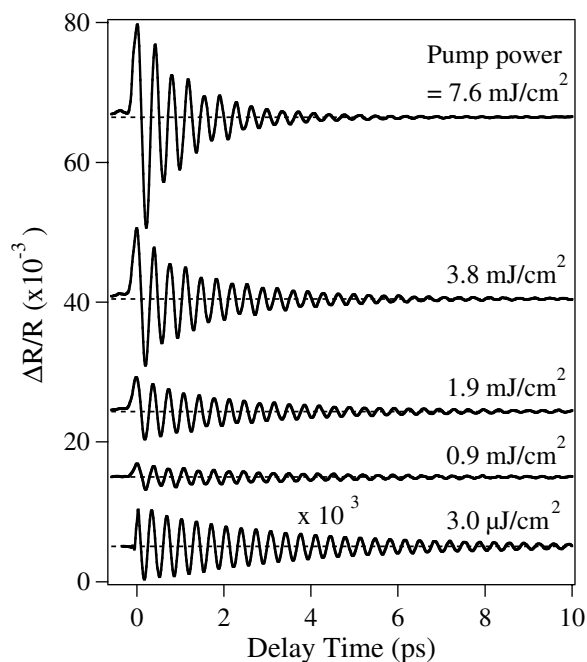


FIG. 1. The transient reflectivity change for Bi at various pump power densities. The dashed lines correspond to the zero level on the reflectivity change of each time-domain signal.

densities. As the pump power density is increased, the peak frequency of the  $A_{1g}$  mode down-shifts and the  $A_{1g}$  mode is asymmetrically broadened to the lower-frequency side. The  $A_{1g}$  mode observed with the seed pulses (bottom of Fig. 2) shows a symmetric line shape with a peak frequency of 2.92 THz. The peak frequency of the  $A_{1g}$  mode linearly decreases from 2.92 to 2.67 THz with increasing the pump power density, as shown in the inset of Fig. 2. This power dependence of the frequency is consistent with the behavior of the frequency shift observed with the pump fluence less than 8.0 mJ/cm<sup>2</sup> [11,14]. However, the magnitude of the frequency shift obtained in our experiment ( $\sim$ 9%) is significantly larger than that observed by DeCamp *et al.* [14] ( $\sim$ 4%). It is surprising that, in addition to the  $A_{1g}$  mode, the  $E_g$  mode appears at 1.61 THz when the pump power density is larger than 3.8 mJ/cm<sup>2</sup>, although the  $E_g$  mode is not usually detected by the isotropic reflectivity ( $\Delta R/R$ ) measurement [5,6]. The observation of the  $E_g$  mode on the  $\Delta R/R$  measurement is explained as follows. The  $A_{1g}$  mode, which has only diagonal non-zero elements in the Raman tensor, has been observed by the  $\Delta R/R$  measurement [5,6]. On the other hand, the  $E_g$  mode, which has only off-diagonal nonzero elements in the Raman tensor, can be detected only by anisotropic reflectivity measurements [7,8]. Thus, the observation of the optical phonon modes is explained on the basis of the first-order Raman tensor  $(\partial\chi)/(\partial Q)$  [9]. We consider that the huge lattice distortion caused by the high density

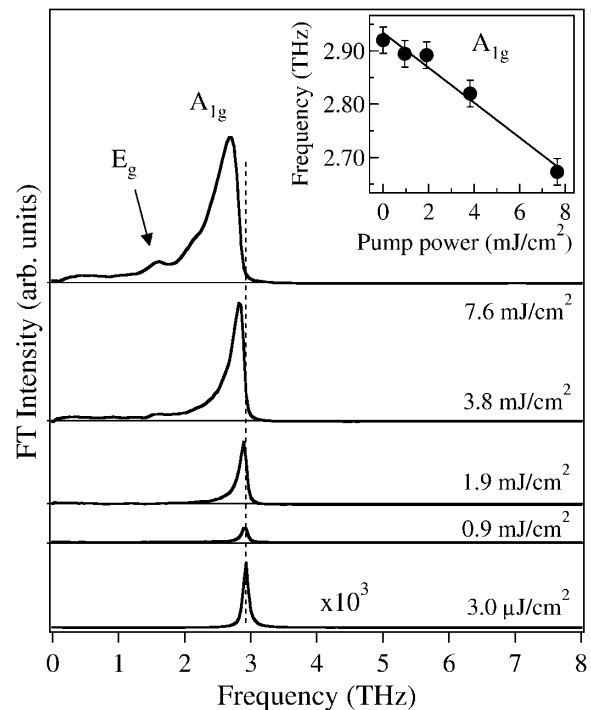


FIG. 2. Fourier transformed spectra obtained from time-domain data in Fig. 1. The dashed line represents the  $A_{1g}$  frequency of 2.92 THz. Inset: the peak frequency of the  $A_{1g}$  mode as a function of the pump power density. The solid line represents a numerical fitting of the data by a linear function.

excitation will modify the lattice symmetry [20], which induces diagonal components in the Raman tensor of the  $E_g$  mode; thus, the large lattice displacement will cause the  $E_g$  mode to be allowed in the  $\Delta R/R$  measurement. The frequency of the  $E_g$  mode observed at  $7.6 \text{ mJ/cm}^2$  is much lower than that obtained using seed pulses (2.16 THz at 300 K). Moreover, broad sidebands appear beside the optical phonon modes. These effects would be due to the strong anharmonic coupling resulting in the hybridization of the optical phonon modes with the two-acoustic phonons [21].

In order to clarify the origin of the frequency shift and the asymmetric line shape of the  $A_{1g}$  mode observed in our experiment, we first attempted to fit the time-domain trace obtained at  $7.6 \text{ mJ/cm}^2$  with a linear combination of two damped harmonic oscillators [5]. As shown in Fig. 3(a), the experimental trace cannot be fitted well with the harmonic oscillator, and there is a large deviation in the phase of the oscillation, which suggests that the mode frequencies are not constant but depend on the time,  $\omega(t)$ . Next, we performed a discrete wavelet transform (DWT) [22] with a variable time window in order to analyze the time

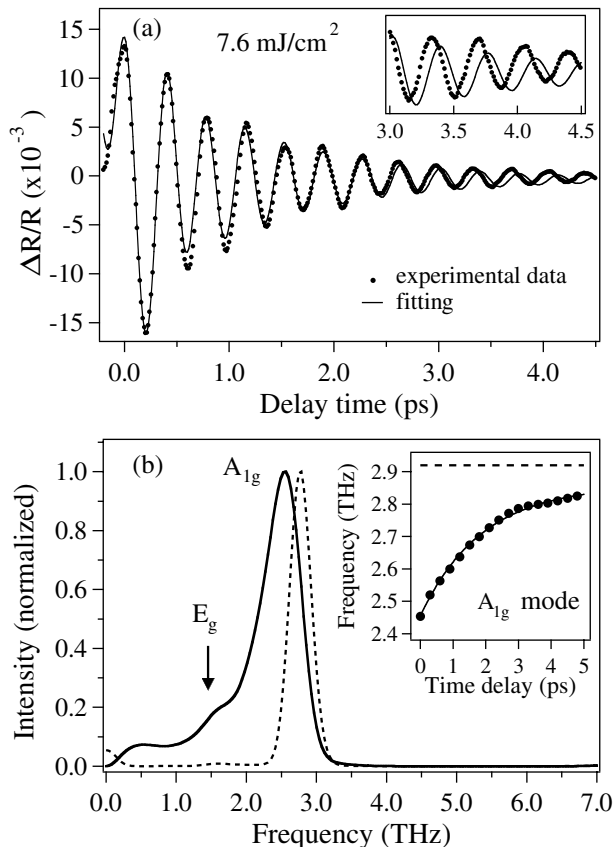


FIG. 3. (a) Numerical fitting of the time-domain trace for  $7.6 \text{ mJ/cm}^2$  with damped harmonic oscillators, showing a large deviation on its phase after 3 ps. (b) DWT spectra obtained for the time delay of 0.3 ps (solid line) and 3.0 ps (dotted line). The inset of (b) shows the variation of the frequency of the  $A_{1g}$  mode as a function of the time delay. The dashed line in the inset represents the ordinary frequency of 2.92 THz.

dependence of the phonon frequency [23]. In Fig. 3(b) we show DWT spectra obtained at  $7.6 \text{ mJ/cm}^2$  for the two time delays of 0.3 ps (second window) and 3.0 ps (tenth window) as examples. The peak frequency of the  $A_{1g}$  mode is 2.52 THz in the second window and 2.78 THz in the tenth window. In the second window, in which the amplitude of the oscillation is quite large, the  $A_{1g}$  mode is asymmetrically broadened to the lower-frequency side and the  $E_g$  mode is broadened to lose its fine structure. The DWT spectrum in the first window shows essentially the same shape as in the second window. Note that in the second window the appearance of the continuum, broad and structureless signal extending to zero frequency, suggests a possibility of transient disordering of the crystal as a precursor of electronic melting and that the line broadening of the optical phonon modes would be due to the strong anharmonic coupling [21]. In the tenth window, only the  $A_{1g}$  mode with a nearly symmetric line shape is observed, and the continuum disappears. The transient frequency of the  $A_{1g}$  mode observed in the DWT spectra with various time windows is plotted as a function of the time delay in the inset of Fig. 3(b). The frequency of the  $A_{1g}$  mode, which is initially down-shifted to 2.45 THz, changes toward the ordinary frequency of 2.92 THz. We suppose from this result that coherent lattice vibrations will initially oscillate with the lower frequency under the anharmonic potential and finally oscillate with the ordinary frequency. The origin of the initial instantaneous frequency change is not lattice heating, because the lattice heating should generally occur on a picosecond time scale [3,24].

In order to analyze the time-dependent phonon frequency, we consider the nonparabolic potential on the basis of classical mechanics [15]. The nonparabolic potential is expressed by  $U(x) = \frac{1}{2}m\omega_0^2x^2 + \frac{1}{3}m\alpha x^3$ , where  $x$  is the atomic displacement,  $m$  is the mass of the oscillator,  $\omega_0$  is the normal frequency of the oscillation with the friction, and  $\alpha$  is a coefficient of the third-order anharmonicity of the potential. The frequency of the anharmonic oscillator in this potential is represented approximately by [15]

$$\omega = \omega_0 + \gamma a^2 \quad \left( \gamma \equiv -\frac{5\alpha^2}{12\omega_0^3} \right), \quad (1)$$

where  $a$  is the amplitude of the oscillation. The value of  $\gamma$  is usually negative because  $\alpha$  is a real number and  $\omega_0$  is positive. Equation (1) implies that the phonon frequency shifts to a lower frequency side than the normal frequency of  $\omega_0$  as the amplitude of the oscillation increases. Figure 4 shows the frequency of the  $A_{1g}$  mode obtained for the pump power density of 7.6 and 1.9  $\text{mJ/cm}^2$  as a function of the squared amplitude of the coherent oscillation. Here, the amplitude of the coherent phonon ( $\Delta R/R_0$ ) was converted into the microscopic amplitude ( $a$ ) by use of a thermodynamic description under the quasiequilibrium system [5]. At 1.9  $\text{mJ/cm}^2$  the  $A_{1g}$  frequency decreases linearly with increasing the squared amplitude. This behavior obeys the relationship given by Eq. (1), accordingly verifying that

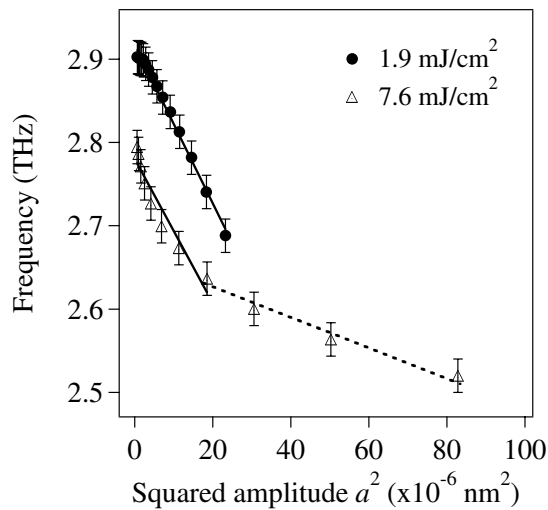


FIG. 4. The variation of the frequency of the  $A_{1g}$  mode for different pump power densities plotted as a function of the squared amplitude of the coherent oscillation. The solid lines indicate the fitting of the data with Eq. (1). The dotted line for  $a^2 \geq 20 \times 10^{-6}$  is a guide for the eye.

the coherent  $A_{1g}$  phonon under the high density excitation has anharmonic character. At the pump power density of  $7.6 \text{ mJ/cm}^2$  the  $A_{1g}$  frequency decreases almost linearly with the same slope as that at  $1.9 \text{ mJ/cm}^2$  for smaller amplitudes than  $20 \times 10^{-6} \text{ nm}^2$ . For the larger amplitudes, the  $A_{1g}$  frequency also shows linear decrease but with a more gradual slope. This suggests a dynamical change of the anharmonic potential due to the large lattice distortion by the high density excitation, which could not be described by the static anharmonic potential [15]. The normal frequency  $\omega_0$  obtained from the fitting at  $7.6 \text{ mJ/cm}^2$  is lower than that at  $1.9 \text{ mJ/cm}^2$ . The origin of this effect is probably the electronic softening, which reduces the oscillation frequency even if the amplitude is quite small [13].

In summary, we have observed the coherent anharmonic phonons in Bi using amplified femtosecond light pulses. The time-domain signal revealed the coherent  $A_{1g}$  phonon with the time-dependent frequency. The analysis based on the DWT method demonstrated that the  $A_{1g}$  frequency depended on the squared amplitude of the oscillation, which is consistent with the behavior of an anharmonic oscillator with a third-order anharmonicity. Moreover, at higher pump power densities, the  $E_g$  mode, in addition to the  $A_{1g}$  mode, was observed, which is explained by the modification of the lattice symmetry under high density photoexcitation. The study of large amplitude coherent phonons will trigger further investigations of precursor phenomena of laser ablation and laser-induced phase transition, as well as nonthermal melting.

We are grateful to the Venture Business Laboratory of Osaka University where the first stage of the experiment was carried out. This work was supported in part by the

Industrial Technology Research Grant Program in 2000 from NEDO of Japan (Grant No. 00X50007x). K.M. is grateful for the support from a Grant-in-Aid for Scientific Research from the Ministry of Education, Culture, Sports, Science, and Technology of Japan.

\*Electronic address: HASE.Muneaki@nims.go.jp

- [1] C. V. Shank, R. Yen, and C. Hirlimann, *Phys. Rev. Lett.* **50**, 454 (1983).
- [2] K. Sokolowski-Tinten *et al.*, *Phys. Rev. B* **58**, R11805 (1998).
- [3] L. Huang *et al.*, *Phys. Rev. Lett.* **80**, 185 (1998).
- [4] C. W. Siders *et al.*, *Science* **286**, 1340 (1999).
- [5] H. J. Zeiger *et al.*, *Phys. Rev. B* **45**, 768 (1992).
- [6] T. K. Cheng *et al.*, *Appl. Phys. Lett.* **57**, 1004 (1990).
- [7] M. Hase *et al.*, *Appl. Phys. Lett.* **69**, 2474 (1996).
- [8] G. A. Garrett *et al.*, *Phys. Rev. Lett.* **77**, 3661 (1996).
- [9] T. Dekorsy, G. C. Cho, and H. Kurz, in *Light Scattering in Solids VIII*, edited by M. Cardona and G. Güntherodt (Springer-Verlag, Berlin, 2000), Chap. 4.
- [10] T. K. Cheng *et al.*, *Appl. Phys. Lett.* **62**, 1901 (1993).
- [11] S. Hunsche *et al.*, *Phys. Rev. Lett.* **75**, 1815 (1995).
- [12] C. J. Brennan and K. A. Nelson, *J. Chem. Phys.* **107**, 9691 (1997).
- [13] P. Tangney and S. Fahy, *Phys. Rev. Lett.* **82**, 4340 (1999).
- [14] M. F. DeCamp *et al.*, *Phys. Rev. B* **64**, 092301 (2001).
- [15] L. D. Landau and E. M. Lifshitz, in *Mechanics*, Course of Theoretical Physics Vol. 1 (Butterworth-Heinemann, Oxford, 1976), 3rd ed., Chap. 5.
- [16] Optical transitions with 800 nm light would occur dominantly at the L point (interband transition). H. Lehmann, in *Landolt-Börnstein, New Series*, edited by O. Madelung (Springer, Berlin, 1983), Vol. 17.
- [17] The electron-hole plasma density of 2% is below the critical density at which nonthermal melting would occur (Ref. [20]).
- [18] J. M. Ziman, *Principle of the Theory of Solids* (Cambridge University Press, London, 1972), 2nd ed.
- [19] S. Takeuchi, *Structure and Physics of Liquid Metals* (Maruzen, Inc., Tokyo, 1978) (in Japanese).
- [20] P. Stampfli and K. H. Bennemann, *Phys. Rev. B* **49**, 7299 (1994).
- [21] J. Ruvalds and A. Zawadowski, *Phys. Rev. B* **2**, 1172 (1970).
- [22] *Proceedings of the International Conference on Wavelet: Time-Frequency Methods and Phase Space, Marseille*, edited by J. M. Combes, A. Grossmann, and Ph. Tchamitchian (Springer-Verlag, Berlin, 1989).
- [23] We chose the Gabor wavelet given by a Gaussian function. The time delay  $\Delta t_n$  was set to be  $0.3(n-1)$  ps ( $n = 1, 2, \dots$ ), where the characteristic time of 0.3 ps corresponds to the average time period of the  $A_{1g}$  oscillation.
- [24] J. Shah, in *Ultrafast Spectroscopy of Semiconductors and Semiconductor Nanostructures*, edited by M. Cardona (Springer Series in Solid-State Sciences (Springer, Berlin, 1996), Chaps. 3–5.